J. Fluid Mech. (1989), *vol.* 201, *pp.* 357–377
Printed in Great Britain

Hydraulic control of zonal currents on a β-plane

By LAURENCE ARMI
Scripps Institution of Oceanography, La Jolla, CA 92093, USA

(Received 13 August 1987 and in revised form 16 August 1988)

Eastward-flowing zonal currents on a thin rotating shell, such as a planetary atmosphere or ocean, have integral properties analogous to open channel flows, the latitudinal width of the zonal current being the analogue of the depth of an open channel flow. The purpose here is to apply the formalism and some of the concepts of open channel flow hydraulics to zonal flows and demonstrate the results with laboratory experiments. In particular a critical relationship is found between a representative zonal velocity, U, and the half-width of the current, a. A dimensionless parameter ($U/\beta a^2$), the Froude/Rossby number, is found analogous to the Froude number of open channel flow. Westward-flowing currents do not have an equivalent analogue.

1. Introduction

Eastward-flowing zonal currents are found on all the major planets explored so far (Jupiter, Saturn and Uranus) as well as in the Earth's atmosphere and oceans. An integral treatment will be presented for these zonal flows. These flows exist in a thin rotating atmospheric or oceanic shell for which the analysis is simplified here to a β-plane. The primary integral property of the flows studied is the energy flux, representing the transport of pressure work rate and kinetic energy of a current with fixed mass transport. It will be seen that the energy flux has a minimum for any given mass flux and that, observationally, many zonal flows are observed at this minimum.

The flows considered will have a primary force balance arising from inertia and variation of the Coriolis force. These are so-called quasi-geostrophic zonal currents on a Rossby β-plane. The effects of friction, although included here, will be considered weak with respect to this primary balance. These flows are then found to be analogous to flows studied in open channel hydraulics in which the primary force balance is between inertia forces and those derived from variation of depth. In what follows it will be seen that the role of the depth in open channel flows is assumed by the width or latitudinal extent of zonal currents. An advantage of an integral approach, such as used here and in the study of open channel flows, is that the final steady state of the flow depends only weakly on the details of the velocity distribution or frictional dissipation within the current. After integration across the current, essential nonlinear aspects of the flow are retained in algebraic form, in particular conditions for critical flow.

Aspects of the analogy between zonal currents and open channel hydraulic flow were pointed out by Rossby (1950) and reviewed by Rex (1950) in consideration of strongly developed 'blocking waves' (cf. Berggren, Bolin & Rossby 1949). In particular, Rossby showed that two dynamically possible states may exist which are compatible with continuity and momentum requirements as in an open channel

hydraulic jump. Similarities in the vorticity equations for large-scale atmospheric motions and small-scale gravity oscillations of a stratified fluid were shown by Ball (1959). The atmospheric flow at 500 mb was compared with theoretical solutions of Long (1955) for flow of a stratified fluid. The type of flow and number of jets formed was seen in the atmosphere to depend on the dimensionless parameter $(U/\beta L^2)$. This is the Rossby β-number introduced by Fultz (1961), the β-plane analogue of the Froude number; it also was found by Rhines (1975) to be important for turbulence on a β-plane. To emphasize the analogy to open channel flow it will be referred to here as the Froude/Rossby number.

A framework similar to that used for the study of open channel flows (cf. Rouse 1950, or Henderson 1966) will be developed here for zonal currents. A true analogue is found between eastward-flowing zonal currents and open channel flows; no true analogue is found for westward-flowing zonal currents. This asymmetry between eastward and westward flows is important and due to the fact that these flows are on a β-plane. The paper begins in §2 with a discussion of the pressure excess which arises from latitudinal variation of the Coriolis force, the zonal current analogue of the hydrostatic pressure for open channel flows. In §3, the energy flux is then found with this pressure excess; properties of the energy flux for zonal currents and open channel flows are compared and contrasted. In §4, the cumulative effects of friction on zonal currents and the tendency for eastward-flowing zonal currents to reach a critical state are discussed. Critical flow and analogous controls for zonal flows are reviewed in §5. Theoretical results are then demonstrated with laboratory observations in §6. A brief early report of this work can be found in Armi (1974).

2. The pressure distribution due to a zonal current

Consider a non-divergent eastward zonal current as illustrated in figure 1 (*a*) with half-width a, and velocity $u(y)$, defined positive to the east. If the flow is geostrophic, the pressure can be obtained by integration of

$$\frac{\partial p}{\partial y} = -\rho f u, \tag{1}$$

where ρ is the density (assumed constant) and f is the variable Coriolis parameter. Then

$$p(y,a) = p_{-a} - \rho f_0 \int_{-a}^{y} u(y')\,\mathrm{d}y' - \rho\beta \int_{-a}^{y} u(y')\,y'\,\mathrm{d}y', \tag{2}$$

where the Coriolis parameter has been expanded such that the current is now considered on a Rossby β-plane. The validity of this expansion, particularly in the neighbourhood of the equator, has been carefully considered by Veronis (1963), Phillips (1966), and Grimshaw (1975).

We shall be considering a steady flow with a total volume transport V, hence a stream function can be defined with

$$\psi(y) = \int_{-a}^{y} u(y')\,\mathrm{d}y'; \quad \psi(-a) = 0, \quad \psi(a) = V. \tag{3}$$

The pressure can then be written

$$p(y,a) = \bar{p}(\psi) + p'(y,a), \tag{4}$$

with

$$\bar{p}(\psi) = p_{-a} - \rho f_0 \psi \tag{5}$$

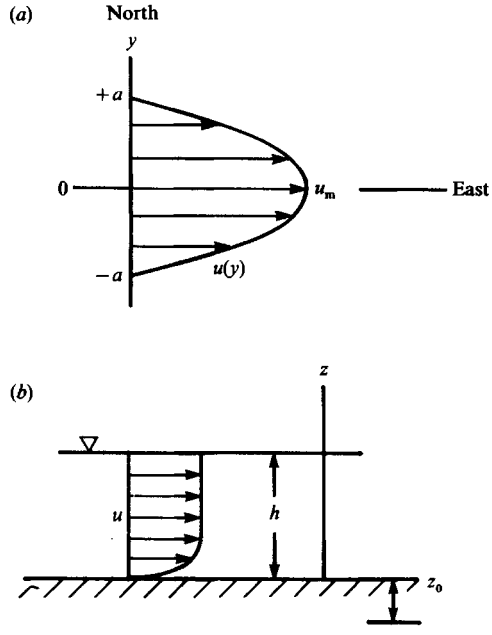

FIGURE 1. (*a*) Plan view for zonal flow, and (*b*) side view for the open channel analogue.

and

$$p'(y,a) = -\rho\beta \int_{-a}^{y} u(y')\, y'\, \mathrm{d}y'. \tag{6}$$

The pressure distribution due to a constant Coriolis parameter f_0, and the pressure at the southern edge of the current, p_{-a}, is $\bar{p}(\psi)$. The pressure excess associated with β, the variation of the Coriolis parameter with latitude, is $p'(y,a)$. Note that $\bar{p}$ is independent of the width of the current whereas p' is not. Rossby (1950) first used the existence of this pressure excess to treat hydraulic-jump-like phenomena or blocking waves in the westerlies.

The pressure excess, p', arises as a result of the current, with volume transport, V, being constrained to flow in a thin rotating shell approximated here by a β-plane. If the transport is as a wide eastward current, the pressure excess on any given streamline will be high, whereas for a narrow faster eastward current with the same transport, the pressure excess on the same streamline will be low.

This pressure excess associated with the geostrophic zonal current is directly analogous to the hydrostatic pressure due to the depth of an open channel flow. To illustrate the analogy, consider the open channel flow shown in figure 1 (*b*). When the hydrostatic approximation applies,

$$\frac{\partial p}{\partial z} = -\rho g, \tag{7}$$

where z is the vertical coordinate and g is the gravitational acceleration; then

$$p(z,h) = \rho g(h-z), \tag{8}$$

where h is the depth measured from the free surface to the bottom. An open channel flow with fixed transport, Q, can either flow as a swift shallow flow with low

hydrostatic pressure along the bottom or as a slow deep current with high hydrostatic pressure along the bottom.

To further illustrate the analogy, assume that the velocity profile of the zonal current is independent of width between $-a$ and $+a$;

$$u(y) = \frac{V}{2a}. \tag{9}$$

The excess pressure is then given by (6) as

$$p'(y,a) = \frac{\rho\beta V}{4a}(a^2 - y^2) \tag{10}$$

and in particular, the excess pressure at the axis ($y = 0$) of the uniform zonal current is

$$p'(0,a) = \rho\frac{\beta V}{4}a. \tag{11}$$

For the open channel flow the pressure at the bottom from (8) is

$$p(0,h) = \rho g h. \tag{12}$$

The role of the gravitational acceleration, g, for open channel flows, is assumed by the term $\frac{1}{4}\beta V$, for the uniform zonal current. It is already worth noting that the magnitude and sign of this term will depend on the magnitude and sign of V, and hence the direction and transport of the zonal current.

The half-width, a, of a zonal current is analogous to the depth, h, for open channel flows. The excess pressure along any streamline for the geostrophic zonal current is a function of the velocity distribution (6) and proportional to the width or latitudinal extent of the current. The sign of the pressure excess is dependent on the flow direction, unlike the bottom pressure in open channel flows.

It is a classical problem in open channel flow hydraulics to determine the flow depth h at various sections along a channel. Specification of the volume flux alone is not adequate to do this; at some location the height must either be specified or established as, for example, at a control section. For zonal flows the width or pressure excess is also not determined by the volume flux alone.

3. The energy flux of a zonal current

The energy flux associated with any zonal current will be defined here as it is for open channel flows (cf. Ippen 1950, p. 507, or Henderson 1966, p. 19). By integration across the current, from $-a$ to $+a$ (figure 1*a*), the flux of kinetic energy plus pressure work rate per unit mass is given by

$$G = \int_{-a}^{a} u\left(\frac{u^2}{2} + \frac{p}{\rho}\right)\mathrm{d}y. \tag{13}$$

With the pressure distribution (4) and stream function (3) given in the previous section, the total energy transport becomes

$$G = \int_{-a}^{a} \tfrac{1}{2}\psi'^3\,\mathrm{d}y - \beta\int_{-a}^{a}\psi'(y)\int_{-a}^{y}\psi'(y)\,y'\,\mathrm{d}y'\,\mathrm{d}y + \frac{p_{-a}V}{\rho} - \tfrac{1}{2}f_0 V^2. \tag{14}$$

As for open channel flows we shall decompose (14) into the specific energy flux, G_0, at the section or longitude in question and terms due to the pressure at $-a, f_0$, and the volume transport V. Then

$$G = G_0 + p_{-a}\frac{V}{\rho} - \tfrac{1}{2}f_0 V^2, \tag{15}$$

with

$$G_0 = \int_{-a}^{a} \tfrac{1}{2}\psi'^3 \,\mathrm{d}y - \beta \int_{-a}^{a} \psi'(y) \int_{-a}^{y} \psi'(y)\, y' \,\mathrm{d}y' \,\mathrm{d}y. \tag{16}$$

Performing the outer integration by parts, assuming a symmetric velocity distribution, (16) can then be written

$$G_0(V, a) = \int_{-a}^{a} (\tfrac{1}{2}\psi'^3 + \beta\psi\psi' y)\,\mathrm{d}y. \tag{17}$$

To apply the specific energy flux to arbitrary zonal velocity distributions, velocity distribution coefficients are used, as in the study open channel flows (cf. Rouse 1950, p. 59 or Henderson 1966, p. 19). Define a velocity distribution function $g(\eta)$ such that

$$u \equiv u_{\mathrm{m}}\, g(\eta), \eta = y/a, \tag{18}$$

with u_{m} the maximum velocity of the zonal current. Define energy, α, and pressure, α', coefficients respectively by

$$\alpha \equiv \int_{-1}^{1} g^3 \,\mathrm{d}\eta \Big/ \left(\int_{-1}^{1} g \,\mathrm{d}\eta \right)^3, \tag{19}$$

$$\alpha' \equiv -\int_{-1}^{1} g \int_{-1}^{\eta} g(\eta')\, \eta' \,\mathrm{d}\eta' \,\mathrm{d}\eta \Big/ \int_{-1}^{1} g^3 \,\mathrm{d}\eta. \tag{20}$$

With a Froude/Rossby number defined by

$$Ro_\beta \equiv \frac{u_{\mathrm{m}}}{\alpha' \beta a^2}, \tag{21}$$

the specific energy flux per unit mass (17) can be written as

$$G_0(V, Ro_\beta) = \left[\frac{(\beta V)^{\frac{2}{3}} \alpha \alpha'^{\frac{2}{3}}}{2} \right] V^{\frac{5}{3}} [(Ro_\beta)^{\frac{2}{3}} + 2(Ro_\beta)^{-\frac{1}{3}}]. \tag{22}$$

For the analogous open channel flow, define the energy or 'Coriolis coefficient' (cf. Henderson 1966, p. 19)

$$\alpha \equiv \frac{1}{h} \int_0^h \left(\frac{u}{U} \right)^3 \mathrm{d}z, \tag{23}$$

where U is defined such that

$$Q = \int_0^h u \,\mathrm{d}z = Uh. \tag{24}$$

The total energy flux per unit mass is given by

$$H = \int_0^h u[\tfrac{1}{2}u^2 + g(h + z_0)] \,\mathrm{d}z. \tag{25}$$

Define the specific energy flux at any section, H_0, independently of the elevation of the bottom, z_0,

$$H = H_0 + Qz_0; \tag{26}$$

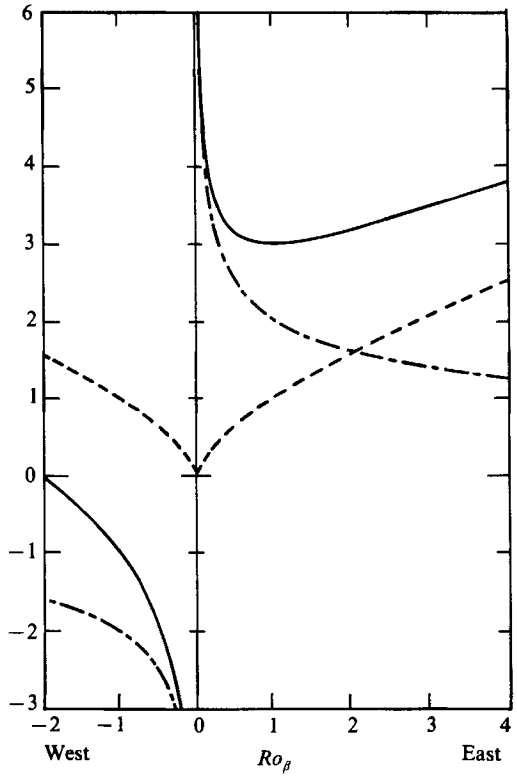

FIGURE 2. Non-dimensional energy flux, G_0' (solid lines) for eastward-flowing, $Ro_\beta > 0$, and westward-flowing, $Ro_\beta < 0$, zonal currents. Contributions due to the kinetic energy flux (dashed lines) and pressure work rate (long and short dashed lines) are also shown. For $Ro_\beta > 0$ the results shown apply also to the open channel analogue with F^2 replacing Ro_β.

then with (24)
$$H_0 = \left[\frac{g^{\frac{2}{3}}\alpha^{\frac{1}{3}}}{2}\right] Q^{\frac{5}{3}}[(F^2)^{\frac{2}{3}} + 2(F^2)^{-\frac{1}{3}}], \tag{27}$$

and the Froude number is defined by
$$F^2 \equiv \frac{\alpha U^2}{gh}. \tag{28}$$

Note the similar role played by the Froude number, F^2, and the Froude/Rossby number, Ro_β, in the specific energy flux equations (22) and (27). (Analogous equations for compressible flows involve the non-dimensional Mach number, M^2.) Just as the Froude number relates inertia forces to pressure forces arising from depth variations of an open channel flow, the Froude/Rossby number relates inertia forces to pressure forces arising from width variations of a zonal current. It is not inconsistent to have $Ro_\beta = O(1)$ and the ordinary Rossby number of the flow small enough such that (1) is applicable. However, at the equator, where $f_0 = 0$, the flow must be strictly two-dimensional and non-divergent.

The non-dimensional specific energy flux, G_0', given by the term with Ro_β of (22)
$$G_0' = (Ro_\beta)^{\frac{2}{3}} + 2(Ro_\beta)^{-\frac{1}{3}} \tag{29}$$
is shown in figure 2 for eastward- and westward-flowing zonal currents. Contributions due to the fluxes of kinetic energy and pressure work rate (potential energy) are

shown separately. For positive values of Ro_β, or eastward flow, the curves shown also apply equally well to the open channel analogue (27); simply substitute F^2 for Ro_β. The usual presentation in open channel flow texts is, however, with non-dimensional depth rather than the Froude number.

4. Subcritical and supercritical zonal currents, effects of weak dissipation

With the volume transport of an eastward zonal flow fixed, figure 2 illustrates that for a broad slow subcritical current with $Ro_\beta < 1$, the pressure work rate, due to a large pressure excess associated with the broad flow, will be large. However, the flux of kinetic energy will be small. Conversely, for a fast, narrow supercritical current with $Ro_\beta > 1$, the pressure work rate is small and the flux of kinetic energy high. The Froude/Rossby number was defined (see (21)) such that the specific energy flux due to the combined flux of kinetic and potential energy (pressure work rate) is a minimum for $Ro_\beta = 1$. Interestingly, no such minimum exists for westward flows; the specific energy flux simply increases with increasing speed of the westward flow. The particular Froude/Rossby number, or alternatively the combination of width and velocity, which makes the specific energy a minimum for a certain volume flux V, was defined by analogy to open channel flows to be the critical Froude/Rossby number.

Rewriting (21) for Ro_β in terms of the volume transport,

$$V = u_m a \int_{-1}^{1} g \, d\eta, \tag{30}$$

gives the relationship between the Froude/Rossby number and the half-width

$$Ro_\beta = \left[\frac{V}{\alpha' \left(\int_{-1}^{1} g \, d\eta \right) \beta} \right] a^{-3} \tag{31}$$

and the Froude/Rossby number and the maximum velocity

$$Ro_\beta = \left[\frac{\left(\int_{-1}^{1} g \, d\eta \right)^2}{\alpha' V^2 \beta} \right] u_m^3. \tag{32}$$

For a fixed transport, u_m is proportional to the cube root of the Froude/Rossby number and the width, a, is inversely proportional to the cube root of Ro_β.

The downstream effects of dissipation, with volume flux conserved, can be immediately seen from figure 2; frictional dissipation can only tend to reduce the specific energy flux. For a supercritical eastward-flowing current, $Ro_\beta > 1$, frictional dissipation will reduce G_0, implying a reduction also of the velocity and widening of the current (31) and (32). For a subcritical eastward-flowing zonal current, $Ro_\beta < 1$, the effects of frictional dissipation are quite opposite to those for a supercritical flow. Dissipation will *increase* Ro_β with an associated *acceleration* and *narrowing* of the current.

The integral properties of interest here are only weakly dependent on the velocity distributions of the zonal flows considered. As examples, α' in the definition of the Froude/Rossby number (20) and (21) and u_m, the maximum velocity at critical

flow ($Ro_\beta = 1, u_m = \alpha'\beta a^2$) from (32), are given below for the following velocity distributions:

uniform $u(y) = u_m$ $\alpha' = 0.33$ $u_m = 0.44\beta^{\frac{1}{3}}V^{\frac{2}{3}}$, (33*a*)

parabolic $u(y) = u_m\left[1-\left(\frac{y}{a}\right)^2\right]$ $\alpha' = 0.25$ $u_m = 0.52\beta^{\frac{1}{3}}V^{\frac{2}{3}}$, (33*b*)

triangular $u(y) = u_m\left[1-\left|\frac{y}{a}\right|\right]$ $a' = 0.23$ $u_m = 0.62\beta^{\frac{1}{3}}V^{\frac{2}{3}}$. (33*c*)

5. Critical flow and control

So far both V, the transport, and G_0, the specific energy, have been prescribed initially and we have discussed how G_0 would change under the influence of friction. This discussion would also apply to the open channel analogue for Q and H_0. In open channel flow there is a further underlying problem of great interest: namely, given the flow rate Q, what determines the specific energy H_0 and hence the relationship of depth to velocity? This is the control problem: controls are features of open channels which tend to produce critical flow and hence a relationship between depth and velocity. Contractions and overflows are common examples of open channel controls.

We shall by analogy to the open channel case illustrate the nature of controls or transitions for zonal currents. In the neighbourhood of a control the role of friction will be assumed to be quite weak. Differentiating the energy equation (15) in the direction of flow gives

$$\frac{dG_0}{dx}+\frac{V}{\rho}\frac{dp_{-a}}{dx} = 0. \tag{34}$$

We have assumed the central latitude of the current remains fixed, dissipation is weak, the flow rate, V, is fixed and dp_{-a}/dx is gradually varying only in the flow direction, x, such that variations in y, the cross stream direction, may be neglected. Rewriting (34) as

$$\frac{dRo_\beta}{dx}\frac{dG_0}{dRo_\beta}+\frac{V}{\rho}\frac{dp_{-a}}{dx} = 0, \tag{35}$$

and with (22) we have

$$-\frac{dRo_\beta}{dx}\left[\frac{(\beta V)^{\frac{2}{3}}\alpha\alpha'^{\frac{2}{3}}}{3}\right]V^{\frac{5}{3}}Ro_\beta^{-\frac{4}{3}}[1-Ro_\beta]+\frac{V}{\rho}\frac{dp_{-a}}{dx} = 0. \tag{36}$$

Solving (36) we have $$\frac{dRo_\beta}{dx} = \left[\frac{(\beta V)^{\frac{2}{3}}\alpha\alpha'^{\frac{2}{3}}}{3}\right]^{-1}V^{-\frac{2}{3}}\frac{Ro_\beta^{\frac{4}{3}}}{[1-Ro_\beta]}\frac{dp_{-a}}{\rho\,dx}. \tag{37}$$

It is noteworthy that the Froude/Rossby number plays a critically important part in (37). We could have just as well solved for either the velocity, u_m, or half-width, a, using (31) and (32). Also note that (37) is the solution in differential form of the quasi-linear equation, (36); the solution is for the non-dimensional dependent variable, Ro_β, as a function of the independent variable, dp_{-a}/dx. However, solutions will exist only if $[1-Ro_\beta] \neq 0$, or if in the neighbourhood of locations where $[1-Ro_\beta] = 0$ certain regularity conditions are satisfied. For this problem it will be that $dp_{-a}/dx = 0$. Locations where $[1-Ro_\beta] = 0$ will be called controls by analogy to open channel flow since they establish unique solutions.

If the flow is subcritical, $Ro_\beta < 1$, then the denominator of (37), $[1-Ro_\beta] > 0$. A

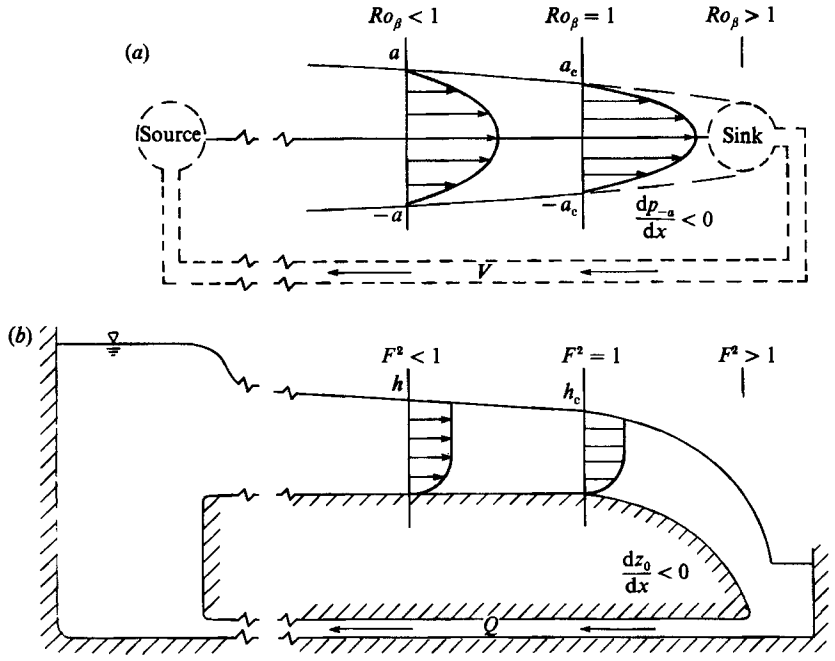

FIGURE 3. (*a*) Plan view of the controlled zonal flow with a source and sink and a constant-flow-rate pump. (*b*) Open channel analogue with a broad-crested weir and a constant-flow-rate pump.

decrease in pressure along the southern edge of the zonal flow will result in a *decrease* of Ro_β to an even lower subcritical value. The flow will slow and broaden, conserving volume transport. For the subcritical open channel analogue, deepening of the channel bottom along the direction of flow also results in a slower and deeper flow with lower Froude number.

In contrast, if the flow is initially supercritical, $Ro_\beta > 1$, then the denominator of (37), $[1-Ro_\beta] < 0$. A decrease in pressure along the southern edge of a supercritical zonal flow then results in a further *increase* in Ro_β. The flow will accelerate and become narrow, just as the supercritical open channel flow analogue accelerates down the side of an overflow.

Now consider the zonal flow shown in figure 3(*a*) and its open channel flow analogue depicted in figure 3(*b*). Figure 3(*a*) is the configuration of a source and sink later studied in a laboratory β-plane. Figure 3(*b*) shows the common open channel flow from a reservoir over a long broad-crested weir; this problem is discussed in many standard texts (cf. Henderson 1966, p. 211). For both problems the volume flow rate, V or Q, is fixed; we shall search for a controlled state.

Assume, since it is observed, that a steady-state solution exists and that it is asymmetric. In the open channel case this means that the flow is *over* the broad-crested weir from the left-hand reservoir to the right-hand reservoir. Only one asymmetric solution exists for flow over the broad-crested weir. The Froude number of this flow is unity at the brink of the weir where dz_0/dx changes from zero to less than zero. No other solution can be asymmetric about $dz_0/dx = 0$, as inspection of the analogue to (36) easily shows. Upstream of the end of the weir, the assumed weak effects of friction will require that the Froude number decrease slightly from unity; in the language of hydraulic engineering this effect on the free surface level is known as a backwater curve.

For the zonal flow of figure 3(*a*), in the immediate neighbourhood of the sink $dp/dx < 0$ and hence $dp_{-a}/dx < 0$, owing to the suction of the constant-flow-rate pump. Upstream of the sink $dp_{-a}/dx = 0$. We shall analyse this problem including the effects of weak dissipation, D. Equation (34) then becomes

$$\frac{dG_0}{dx} + \frac{V}{\rho}\frac{dp_{-a}}{dx} = -\frac{V}{\rho}D \tag{38}$$

and its solution (37) becomes

$$\frac{dRo_\beta}{dx} = \left[\frac{(\beta V)^{\frac{2}{3}}\alpha\alpha'^{\frac{2}{3}}}{3}\right]^{-1} V^{-\frac{2}{3}}\frac{Ro_\beta^{\frac{4}{3}}}{[1-Ro_\beta]}\left[\frac{dp_{-a}}{dx}+D\right]. \tag{39}$$

From (39) we see that when $dp_{-a}/dx = 0$ the effects of frictional dissipation are as discussed in the previous section. For initially subcritical flows, dissipation raises Ro_β whereas for initially supercritical flows, dissipation decreases Ro_β. The minimum for G_0 occurs for $Ro_\beta = 1$, critical flow.

Over most of the flow $dp_{-a}/dx = 0$ and $D > 0$; hence over most of the flow, $[(dp_{-a}/dx)+D] > 0$. However, in the immediate neighbourhood of the sink $dp_{-a}/dx < 0$ and with weak dissipation $[(dp_{-a}/dx)+D] < 0$. Our concern will now be with the location where $[(dp_{-a}/dx)+D] = 0$. From (38) it follows that at this location, either [$Ro_\beta \neq 1$ and $dRo_\beta/dx = 0$] or [$Ro_\beta = 1$ and $dRo_\beta/dx > 0$].

The first possibility represents either an entirely supercritical flow or an entirely subcritical flow in the neighbourhood of $[dp_{-a}/dx)+D] = 0$. The flow is then symmetrical about this location since $[1-Ro_\beta]$ is everywhere either greater or less than zero. An initially subcritical flow will increase in speed for $[(dp_{-a}/dx)+D] > 0$ and decrease in speed as $[(dp_{-a}/dx)+D] < 0$. An initially supercritical flow behaves in exactly the opposite but symmetrical way about $[(dp_{-a}/dx)+D] = 0$. For $[(dp_{-a}/dx)+D] > 0$ the supercritical flow will decrease in speed and increase again as $[(dp_{-a}/dx)+D] < 0$.

Only the second possibility, namely $Ro_\beta = 1$ and $dRo_\beta/dx > 0$, where $[(dp_{-a}/dx)+D] = 0$ is associated with an asymmetric flow. The flow is so-called 'controlled' because at the control location, $[dp_{-a}/dx)+D] = 0$, a relationship between velocity and width is established through $Ro_\beta = 1$. For the open channel analogue of figure 3(*b*), the analogous relation between velocity and depth is established by $F^2 = 1$.

6. Experiments

Some aspects of the open channel analogue for zonal currents can be demonstrated with laboratory experiments. The experiments were performed on the 210 cm diameter rotating table at the Woods Hole Oceanographic Institution. A brief description and photographs of the facility are presented by Faller (1960) and a more detailed description is given by Ibbetson & Phillips (1967). The experimental arrangement is best seen in figure 4. A source and sink were used to create the zonal currents. The sink was a small pump of up to 300 ml s^{-1} capacity which discharged through a diffused source. A barrier at 0° longitude extended from the outer wall to the centre of the tank and separated the source and sink. The basin formed is thus of 360° longitudinal extent. In addition to radial longitude lines at 30° intervals, the distance to the centre of the tank is marked at 10 cm intervals. The source and sink were placed 85 cm from the centre of the tank.

All flows were visualized using the thymal blue technique of Baker (1966). Dye was

formed along radial wires at a height 4 cm above the bottom. Each radial wire had 3.5 cm long vertical wires soldered at their centres to the radial wire every 5 cm along the radius. The combination of radial and vertical wires was chosen in order to visualize both azimuthal and radial displacements. No significant radial motions were observed from the dye releases of the vertical wires, confirming the strictly zonal behaviour of the flows. Quantitative measurements of velocity were made from the Lagrangian displacement of dye formed at the radial wires.

With rapid rotation, much of the centre of the tank was actually dry; for example in figures 4, 5, 7, 10 and 11 the parabolic free surface intersects the bottom at a radius of 50 cm. The radial wires were suspended 4 cm off the table bottom; hence dye is only visible at radii for which the water depth is deeper than 4 cm. For example in figures 4, 5, 7, 10 and 11 the dye is visible only at radii larger than 70 cm. The water depth at the radius of the source and sink was maintained at 10 cm.

After discussion of the laboratory β-plane (§6.1) controlled flows are discussed in §6.2. Supercritical flows, both eastward and westward, are discussed in §6.3. All of the above flows were steady. In order to study the application of Rossby wave dynamics, impulsively started flows are discussed in §6.4. These flows also reach a steady state after passage of the Rossby waves.

6.1. *The laboratory β-plane*

Another way of looking at this problem is in terms of the total vorticity equation integrated over the depth:

$$\frac{\mathrm{d}}{\mathrm{d}t}(\xi+f) = \boldsymbol{u}\cdot\nabla\xi + v\beta + \frac{w_\mathrm{e}}{D}f = 0, \tag{40}$$

where ξ, the relative vorticity, is assumed $\ll f$, the planetary vorticity, $\boldsymbol{u}$, is the velocity field, D is the depth, and $(w_\mathrm{e}/D)f$ is the vortex stretching due to Ekman pumping on the bottom. Horizontal friction has been neglected relative to bottom friction.

For laboratory flows the role of β, the variation of planetary vorticity, can be replaced by variations of the depth, D, with radial distance from the centre of the tank, r,

$$\beta = -f\frac{\mathrm{d}D}{D\,\mathrm{d}r}. \tag{41}$$

In these experiments depth variations are given by a parabolic free surface with

$$\frac{\mathrm{d}D}{\mathrm{d}r} = \frac{\omega^2 r}{g}, \tag{42}$$

where ω is the rotation rate; then

$$\beta = \frac{-2\omega^3 r}{gd}. \tag{43}$$

The laboratory equivalent of north was towards the shallow centre; the large diameter outer rim was the deep south.

Scaling the vorticity equation with the half-width, a, the characteristic steady velocity, u_m, and the zonal scale, L, gives the non-dimensional steady vorticity equation:

$$\left[\frac{u_\mathrm{m}}{\beta a^2}\right]\boldsymbol{u}\cdot\nabla\xi + v + \left[\frac{E^{\frac{1}{2}}fL}{\beta a^2}\right]\xi = 0. \tag{44}$$

The Ekman pumping term is now given by

$$\frac{w_e}{D}f = \left[E^{\frac{1}{2}}\frac{u_m}{a}f\right]\xi, \tag{45}$$

with the Ekman number, E, defined by (cf. Veronis 1973)

$$E \equiv \frac{2\nu}{fD^2}. \tag{46}$$

When $[u_m/\beta a^2] \ll 1$, the flow is very subcritical and frictionally controlled. The dynamics of (44) is linear and solvable in terms of the strength of source and sink distributions. This problem has been treated by Faller (1960); the appropriate equation is simply

$$\frac{\partial\psi}{\partial x} + \left[\frac{E^{\frac{1}{2}}fL}{\beta a^2}\right]\nabla^2\psi = 0. \tag{47}$$

For the very supercritical case, $[u_m/\beta a^2] \gg 1$, the effects of variation of planetary vorticity are weak. This problem was treated by Gadgil (1971) with the predictive equation

$$\frac{d\xi}{dt} = -\left[\frac{E^{\frac{1}{2}}fL}{u_m}\right]\xi. \tag{48}$$

The zonal currents treated here are those for which the vorticity equation is nonlinear, i.e. $[u_m/\beta a^2] \sim 1$; the vorticity equation is then of higher order and additional information is needed to obtain a solution. The critical condition $Ro_\beta = 1$ at a control provides a relation between u_m and a to complete the solution.

For the laboratory experiments the magnitude of frictional effects due to Ekman pumping on the bottom is given in (44) by the term

$$\epsilon_L \equiv \left[\frac{E^{\frac{1}{2}}fL}{\beta a^2}\right]. \tag{49}$$

The effects of friction over lengthscales comparable with the half-width are then given by

$$\epsilon_a \equiv \left[\frac{E^{\frac{1}{2}}f}{\beta a}\right] = \left[\frac{\nu^{\frac{1}{2}}g}{\omega^{\frac{5}{2}}ra}\right]. \tag{50}$$

For most of the experiments $\epsilon_a \sim 0.04$ and $\epsilon_L \sim 4$ based on the tank circumference at the radius of the current. Frictional effects were important over the total circumferential length separating the source and sink on the rotating table, yet frictional effects were small at lengthscales of order the half-width of the zonal currents studied.

The Rossby number

$$Ro = \frac{u_m}{\omega a} \tag{51}$$

of the currents studied was small, typically $Ro \sim 0.06$. Although the table was not covered, the vertical barrier at 0° longitude spun up the air immediately above the table. Drift velocities induced by the remaining wind stress at the free surface were only of order 0.02 cm s^{-1}.

6.2. *Controlled flows*

Two examples of flows with control near the sink are shown in figures 4 and 5. These are photographs of the configuration sketched in figure 3(*a*). The sink is on the left

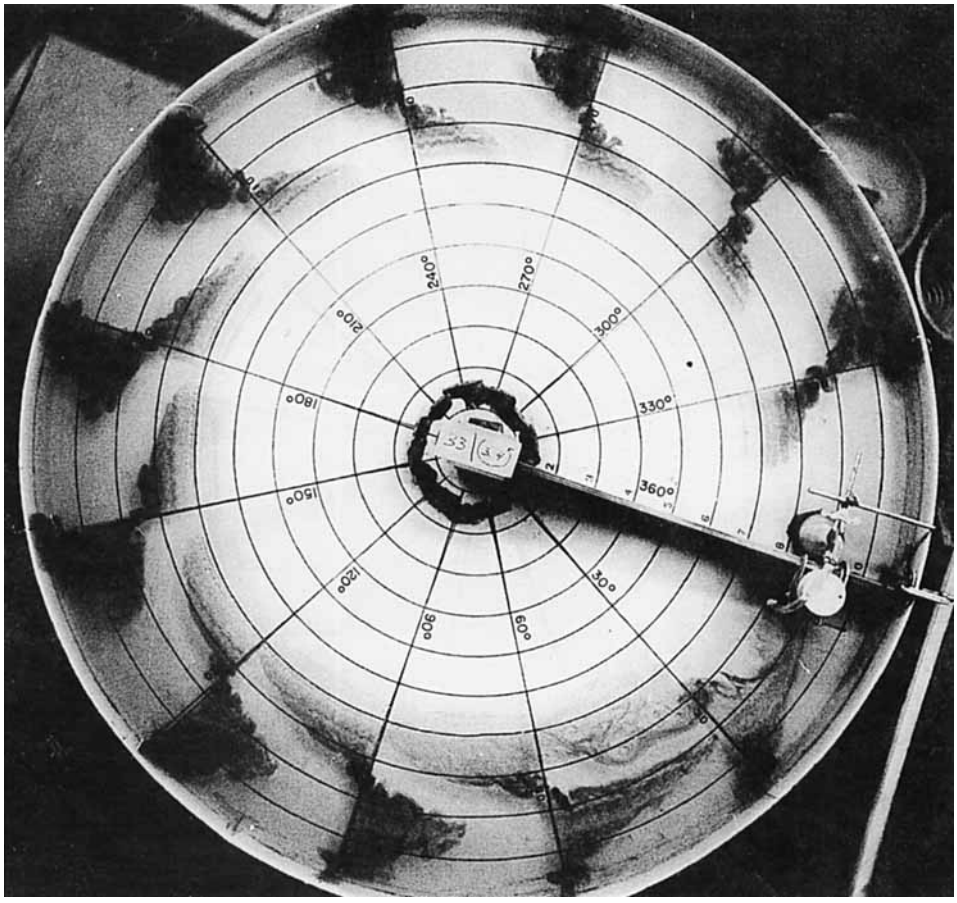

FIGURE 4. Top view of eastward zonal flow established by a source and sink to the east and west respectively of a vertical barrier at 0° longitude. For this flow $\tau = 3.4$ s (counterclockwise), $\beta = 0.11$ cm^{-1} s^{-1}, $V = 7$ cm^2 s^{-1}, $T = 40$ s, $u_m = 0.8$ cm s^{-1}, $Ro_\beta = 0.9$, $\epsilon_a = 0.04$. The free surface intersects the bottom at a radius of 50 cm and the depth is less than 5 cm at radii less than 70 cm.

side of the barrier at 0° longitude and since the table is rotating clockwise, as viewed from above, the flow is eastward. For the flow rates measured, 7 cm^2 s^{-1} and 16 cm^2 s^{-1} respectively, critical half-widths (equation (33*b*)) are 6 cm and 8 cm respectively for figures 4 and 5. Since these widths are less than the available half-width on the rotating table (about 15 cm for this rotation rate), controlled flows are established in the neighbourhood of the sink. The two photos would be identical if we were dealing with a purely linear phenomenon since the product of the flow rate per unit depth, V, and the time since the dye release began, T, is approximately equal for both photos. For the lower flow rate ($V = 7$ cm^2 s^{-1}), of figure 4, the zonal currents are narrower than the higher flow rate case ($V = 16$ cm^2 s^{-1}) shown in figure 5.

Experimental results for a number of eastward flows controlled by a sink are summarized in figure 6. Two different rotation periods and hence two different values of β were studied. The velocities were measured from photographs using the dye released at 60° longitude upstream of the sink since the dye released 30° upstream became distorted close to the sink, as can be seen in figure 4. Hence, because of frictional dissipation all the measurements were made in the slightly subcritical

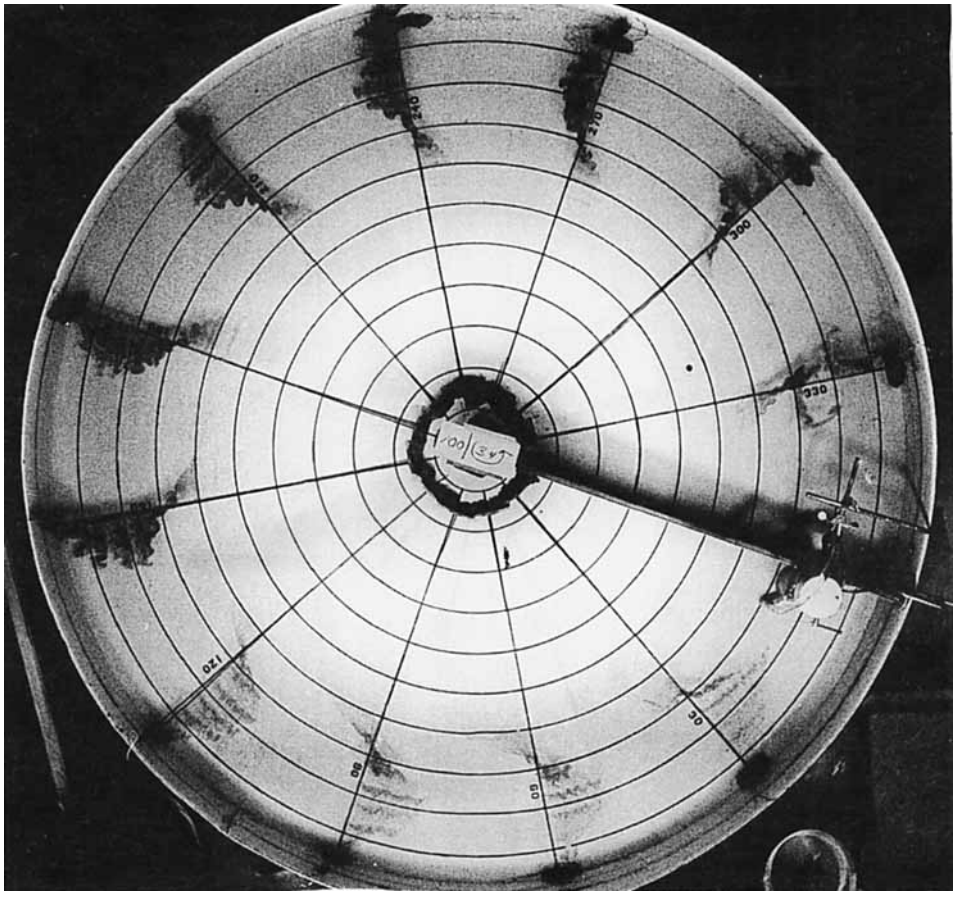

FIGURE 5. Top view of eastward zonal flow as in figure 4, but for this flow $\tau = 3.4$ s (counterclockwise), $\beta = 0.11$ cm^{-1} s^{-1}, $V = 16$ cm^2 s^{-1}, $T = 20$ s, $u_m = 1.1$ cm s^{-1}, $Ro_\beta = 0.7$, $\epsilon_a = 0.03$.

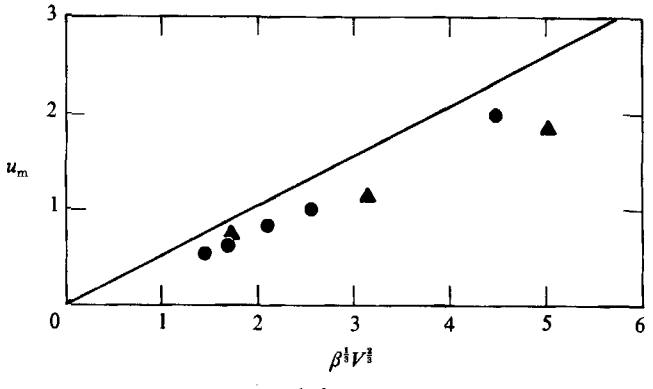

FIGURE 6. Maximum zonal velocity u_m *vs.* $\beta^{\frac{1}{3}}V^{\frac{2}{3}}$ for eastward flows. ●, $\omega = 1.57$ s^{-1}, $\beta = 0.074$ cm^{-1} s^{-1}; ▲, $\omega = 1.85$ s^{-1}, $\beta = 0.11$ cm^{-1} s^{-1}. The line is the theoretical value $u_m = 0.52\beta^{\frac{1}{3}}V^{\frac{2}{3}}$ for a critical parabolic velocity distribution (33*b*).

region upstream of the control. The volume flow, V, was computed from the displacement of the dye line emanating at 60° longitude upstream of the sink. The solid line shown in figure 6 has a slope of 0.52, the value appropriate for a critical parabolic velocity distribution (33*b*). All the measurements are bounded by the critical value.

Although for these experiments, frictional effects were small at lengthscales of order the half-width of the current, they were not negligible over the total circumferential length separating the source and sink on the table. The transport computed for figure 6 includes the pumped flow plus a weak recirculating flow. This recirculating flow is clearly visible in figures 4 and 5 at radii less than 85 cm and 80 cm respectively. At these radii the water depth is shallow: 7.6 cm at a radius of 80 cm decreasing to zero at a radius of 50 cm. The recirculation is due to Ekman pumping on the bottom (equation (49)) and varies with circumferential distance around the table. This recirculating flow was difficult to estimate, but contributed less than 25% to the total transport reported in figure 6. Since the recirculating flow is not directly controlled at the sink, the theoretical result shown in figure 6 will overestimate the observed maximum velocities of the controlled flow alone.

One primary effect of dissipation, anticipated in §3, was that these subcritical flows should speed up in the direction of the flow. This effect is clear in both figures 4 and 5. The dye displacement increases by a factor of two in the direction of the flow, counterclockwise to the east, around the table. Less obvious is an anticipated narrowing of the current. This is masked to some extent by the increasing transport in the flow direction due to Ekman pumping on the bottom.

6.3. *Supercritical flows*

For all westward flows the specific energy flux, G_0', has no minimum, as can be seen by inspection of figure 2. For these westward flows no critical state exists; the Ro_β of the flow is set at the source and they broaden and slow down in the direction of flow. This effect is just opposite to that for eastward subcritical flows, which narrow and speed up in the direction of flow. As will also be demonstrated in the next subsection, long Rossby waves, which propagate information about changes to these flows, can only travel in the direction of these flows and not upstream from a hydraulic control. All westward flows are therefore supercritical.

Examples of these westward flows are shown in figures 7 and 8. Rather than interchange the source and sink, the table was simply rotated clockwise instead of counterclockwise. Hence west is now in the counterclockwise direction. If you prefer, you are now viewing a more familiar clockwise rotation from down under; look at the photos (figures 7 and 8) in a mirror if this is confusing. For the westward flow shown in figure 7 the table is rotating rapidly, as in figures 4 and 5, and hence β is large. Note that in the direction of flow (counterclockwise/west) the flow speed is decreasing in contrast to the eastward flows shown in figures 4 and 5.

For the flows shown in figures 8 and 9, the rotational period of the table was long ($\tau = 7.0$ s) and hence $\beta = 0.02$ cm^{-1} s^{-1} is small. For figure 8 the table was rotating clockwise, for figure 9 counterclockwise. For figure 8 the dye wires were left on for only a short time to produce a single dye line. Both of these flows are supercritical, that shown in figure 8 because it is westward. Although the flow shown in figure 9 is eastward, for this value of β and flow rate, even the broadest flow possible, in this case half the table radius, is supercritical. Note that for this flow $\epsilon = 0.2$, a relatively high value associated with significant entrainment of new fluid into the eastward flow

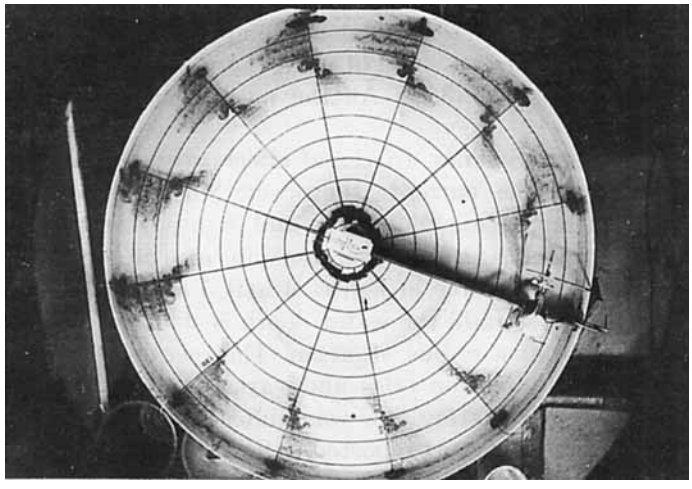

FIGURE 7. Top view of westward zonal flow. The table is now rotating clockwise. $\tau = 3.4$ s (clockwise), $\beta = 0.11$ cm^{-1} s^{-1}, $V = -30$ cm^2 s^{-1}, $T = 40$ s, $u_m = 0.8$ cm s^{-1}, $Ro_\beta = -0.6$, $\epsilon_a = 0.03$.

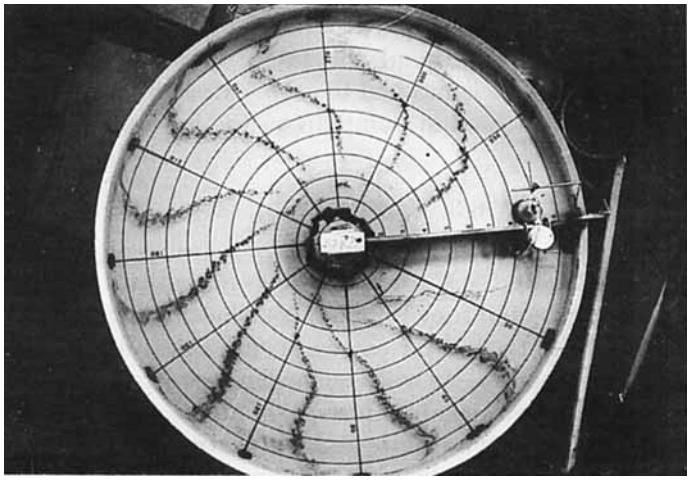

FIGURE 8. Top view of westward zonal flow as in figure 7, but for this flow $\tau = 7.0$ s (clockwise), $\beta = 0.02$ cm^{-1} s^{-1}, $V = -7$ cm^2 s^{-1}, $T = 240$ s, $u_m = -0.2$ cm s^{-1}, $Ro_\beta = -0.2$, $\epsilon_a = 0.09$.

and a compensating westward return flow. The effect of frictional dissipation on the supercritical eastward flow is to broaden the current in the direction of flow.

6.4. *Impulsively started flows and Rossby wave propagation*

The application of Rossby wave dynamics can be demonstrated by impulsively starting these flows. Initially the fluid on the rotating table was spun up and motionless with respect to the table. After starting the pump, two types of waves propagate around the table: Kelvin gravity waves and Rossby waves. The gravity waves are fast and produce a uniform flow at all longitudes; the Rossby waves are slow and produce the velocity distributions seen in the zonal currents.

Figures 10 and 11 show the results of these impulsively started experiments. In both, dye lines were first formed and then the pump was started at $T = 0$. The sequences of photographs were taken at 15 s intervals after the start of the pump. In

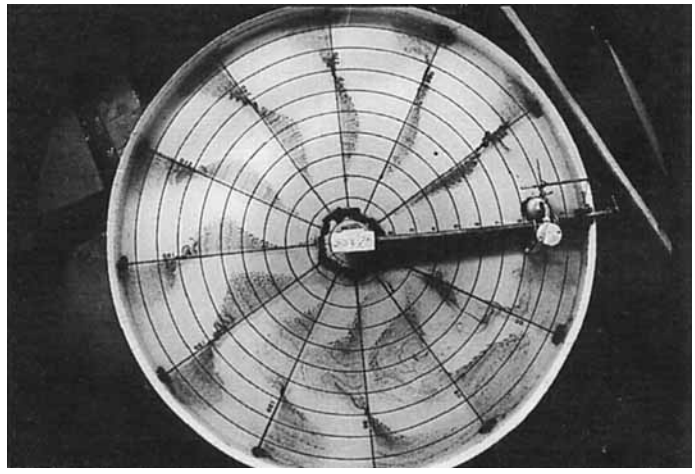

FIGURE 9. Top view of supercritical eastward zonal flow. The table is now rotating counterclockwise, otherwise the configuration and flow rate are identical to the westward flowing current in figure 8. $\tau = 7.0$ s (counterclockwise), $\beta = 0.02$ cm^{-1} s^{-1}, $V = -7$ cm^2 s^{-1}, $T = 60$ s, $u_m = -0.4$ cm s^{-1}, $Ro_\beta = 2$, $\epsilon_a = 0.2$.

figures 10(*a*) and 11(*a*), the uniform flow left behind by the fast moving gravity waves can be seen everywhere except in the immediate neighbourhood of the sink in figure 10(*a*) and the source in figure 11(*a*). Here these sequences differ since figure 10 is for an impulsively started eastward zonal flow while figure 11 is for an impulsively started westward flow.

Since long Rossby waves can only propagate to the west, for the impulsively started eastward flow in figure 10, they propagate upstream from the controlling sink. At 15 s (figure 10*a*) a zonal flow with a parabolic velocity distribution can only be seen at 30° of longitude west of the sink. At 30 s (figure 10*b*) the parabolic distribution has reached 60° of longitude west (clockwise) from the sink; at 45 s the Rossby waves have propagated to approximately 90° west of the controlling sink. The Rossby waves propagate westward and upstream against the flow from the sink with speed $O(\frac{1}{2}\beta a^2)$. This case is analogous to what would happen if the open channel flow shown in figure 3(*b*) were impulsively started. A gravity wave then propagates upstream with information about the hydraulic control with a speed $(gh)^{\frac{1}{2}}$.

The sequence shown in figure 11 is for a westward impulsively started current. The configuration is identical to that shown in figure 10, only the table is now rotating clockwise and west is in the counterclockwise direction. The Rossby waves again propagate to the west (now counterclockwise) in the same direction as the westward flow. Inspection of figure 2 shows that for all westward flows, no minimum exists for the specific energy flux. In fact, since long Rossby waves can only propagate to the west, all eastward flows are in a sense supercritical with respect to long Rossby waves. No long Rossby waves can ever propagate upstream against a westward current, whereas for subcritical ($Ro_\beta < 1$) eastward flows the Rossby waves do propagate upstream. In figure 11(*a*), after 15 s the Rossby waves have been carried with the current approximately 30° westward (counterclockwise) from the source. In figure 11(*b*), after 30 s, the waves have left a parabolic zonal current as far west as approximately 120°.

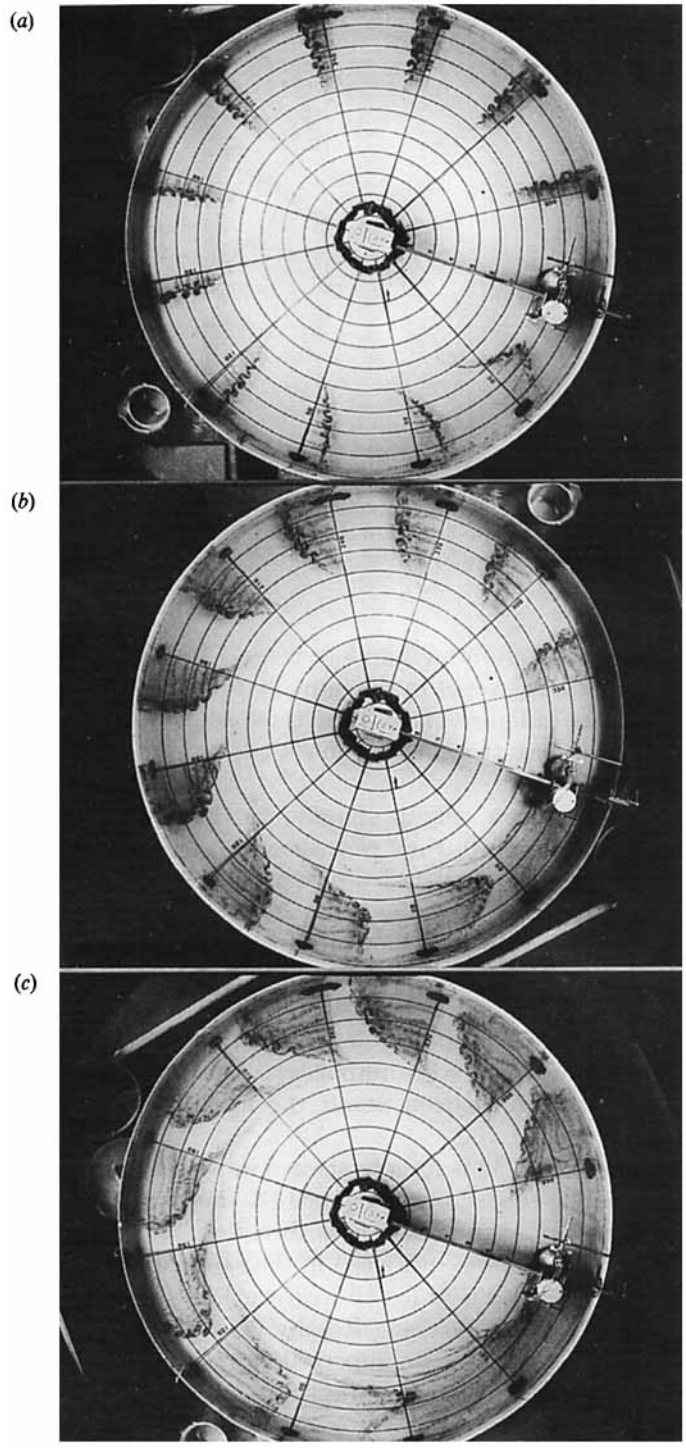

FIGURE 10. Top views of an impulsively started eastward zonal flow. The pump was started at $T = 0$ and the photos are for (*a*) $T = 15$ s, (*b*) 30 s, (*c*) 45 s. $\tau = 3.4$ s (counterclockwise), $\beta = 0.11$ cm^{-1} s^{-1}, $V = 30$ cm^2 s^{-1}. Note the westward (clockwise) Rossby wave propagation from the controlling sink. The free surface intersects the bottom at a radius of 50 cm and the depth is less than 50 cm at radii less than 70 cm.

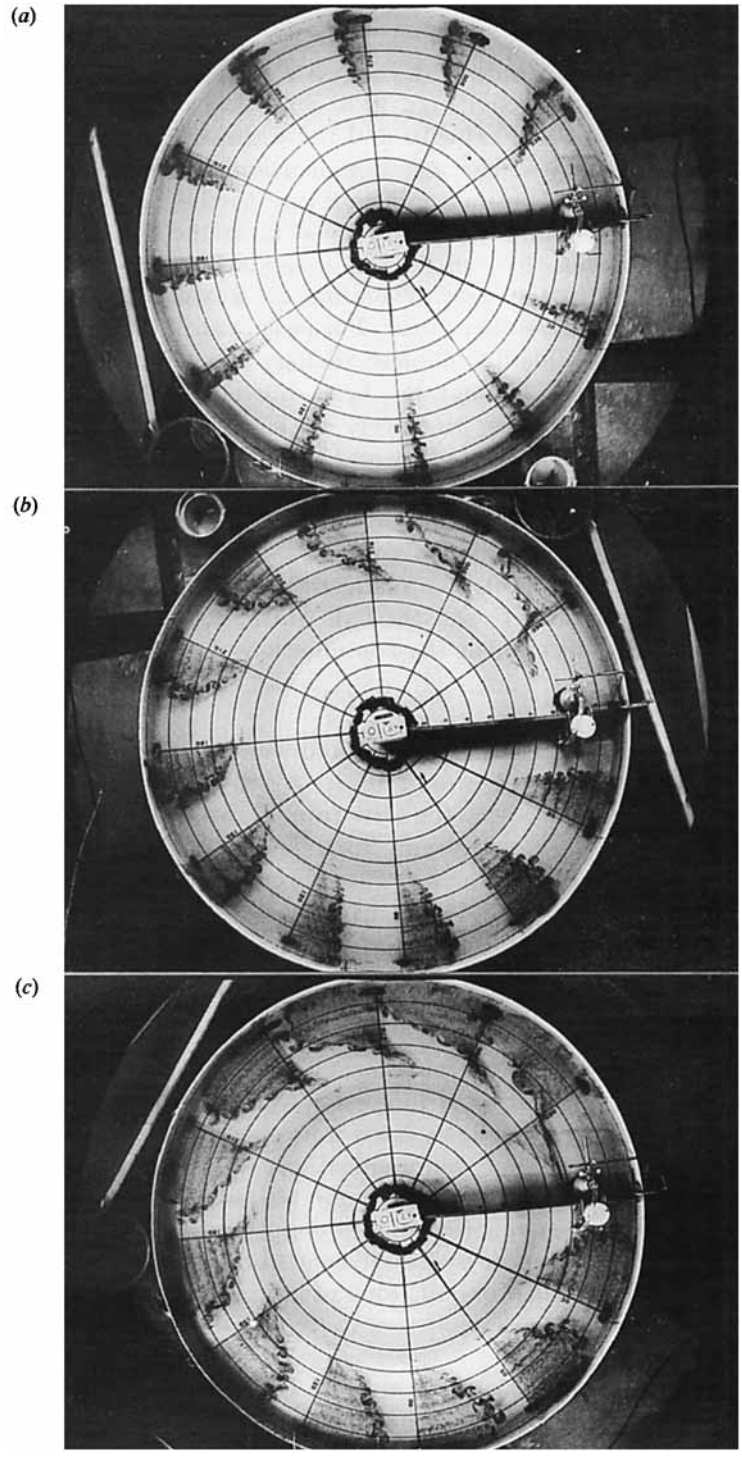

FIGURE 11. Top views of an impulsively started westward zonal flow. The table is now rotating clockwise, otherwise everything is identical to the configuration for the impulsively started eastward zonal flow of figure 10. The pump was started at $T = 30$ s, and the photos are for (*a*) $T = 15$ s, (*b*) 30 s, (*c*) 45 s. $\tau = 3.4$ s (clockwise), $\beta = 0.11$ cm^{-1} s^{-1}, $V = 30$ cm^2 s^{-1}. Note the westward (counterclockwise) Rossby wave propagation from the source.

7. Conclusions

The concept of hydraulic control, developed for open channel flows, applies to zonal flows on a β-plane. In particular, at a control, a critical relationship exists between a representative zonal velocity and the width of the current. This critical relationship can be expressed through a dimensionless parameter, the Froude/Rossby number (21) defined in an analogous way to the Froude number of open channel flow. For the hydraulic control of zonal flows the flow direction is crucial since long Rossby waves, by which the information concerning the control propagates, only travel to the west. Therefore all westward flows are controlled upstream and are in a sense supercritical. For eastward flows both subcritical and supercritical flows are possible in complete analogy to open channel flow.

Throughout the paper the analogy has been drawn with open channel flows for both simplicity and convenience. However, in the light of the similarities in the vorticity equations for flows on a β-plane and stratified flows shown by Ball (1959), a more direct comparison for the laboratory experiments might have been with selective withdrawal from a stratified reservoir (cf. Yih 1980, pp. 106–122) for which a critical Froude number criterion also applies.

The flows considered were barotropic and a critical relationship was found to apply between velocity or flow rate, V, and the half-width, a, for these zonal flows. In a stratified and rotating environment the combination of a critical criterion

$$F = V/d^2N$$

for the depth of the flow d, given the Väisälä frequency N (cf. Yih 1980, p. 116), with the criterion found here, $Ro_\beta = 1$, would apply.

In the treatment presented here the flow rate, V, was specified and the specific energy flux per unit mass, G_0, was found, (22). The problem can always be turned around; given G_0 and solving for the flow rate through the critical flow relationship $Ro_\beta = 1$, (21).

Some possible extensions of the concept of hydraulic control of zonal flows introduced here are the following: throughout the discussion, the centre latitude (f_0), of the current was assumed fixed. However, non-zonal flows, for example those moving north or south along a coast, could be treated with (15). Now the term $\frac{1}{2}f_0V^2$ is an additional topographic forcing term like $p_{-a}V/\rho$ and would be included in (34). Since the integral properties of interest were only weakly dependent on the velocity distributions of the zonal flows, a few were chosen, (33a, b, c), for illustration. However, J. Willebrand (personal communication) suggested and showed that the specific energy flux, G_0, can be minimized for all possible velocity distributions. Although the flows were treated here using the simplification of the β-plane it will be essential to extend the concept of hydraulic control to spherical geometry for flows extending over large latitudinal extent, for example the differential rotation of the Sun.

This work was begun at the Geophysical Fluid Dynamics Summer Study Program at the Woods Hole Oceanographic Institution in 1974. The program was sponsored by the National Science Foundation. Thanks to Melvin Stern for telling me about the obscure paper of Rossby (1950) and subsequent stimulating discussions. I received many helpful comments, particularly from Jürgen Willebrand, Larry Pratt, Michael McIntyre, Tony Maxworthy and Jack Whitehead. My research is supported by the Office of Naval Research and the National Science Foundation.

REFERENCES

ARMI, L. 1974 An energy minimization principle for oceanic currents and atmospheric jet streams. *Geophys. Fluid Dyn. Notes, WHOI Ref.* 74-63(2), 1–14.

BAKER, D. J. 1966 A technique for the precise measurement of small fluid velocities. *J. Fluid Mech.* **26**, 573–575.

BALL, F. K. 1959 Long waves, lee waves and gravity waves. *Q. J. R. Met. Soc.* **85**, 24–30.

BERGGREN, R., BOLIN, B. & ROSSBY, C.-G. 1949 An aerological study of zonal motion, its perturbations and breakdown. *Tellus* **1**, 14–37.

FALLER, A. J. 1960 Further examples of stationary planetary flow patterns in bounded basins. *Tellus* **12**, 159–171.

FULTZ, D. 1961 Developments in controlled experiments on larger scale geophysical problems. *Adv. Geophys.* **7**, 1–103.

GADGIL, S. 1971 Structure of jets in rotating systems. *J. Fluid Mech.* **47**, 417–436.

GRIMSHAW, R. H. J. 1975 A note on the beta-plane approximation. *Tellus* **27**, 351–357.

HENDERSON, F. M. 1966 *Open Channel Flow*, pp. 522. Macmillan.

IBBETSON, A. & PHILLIPS, N. 1967 Some laboratory experiments on Rossby waves in a rotating annulus. *Tellus* **19**, 81–87.

IPPEN, A. T. 1950 Channel transitions and controls. *Engineering Hydraulics, Proc. Fourth Hydraulics Conference, Iowa Inst. of Hydraulic Res., June 12–15, 1949* (ed. H. Rouse), pp. 496–588. Wiley.

LONG, R. R. 1955 Some aspects of the flow of stratified fluids. III. Continuous density gradients. *Tellus* **7**, 341–357.

PHILLIPS, N. A. 1966 The equations of motion for a shallow rotating atmosphere and "the traditional approximation". *J. Atmos. Sci.* **23**, 626–628.

REX, D. F. 1950 Blocking action in the middle troposphere and its effect upon regional climate. I. An aerological study of blocking action. *Tellus* **2**, 196–211.

RHINES, P. B. 1975 Waves and turbulence on a beta-plane. *J. Fluid Mech.* **69**, 417–443.

ROSSBY, C.-G. 1950 On the dynamics of certain types of blocking waves. *J. Chinese Geophys. Soc.* **2**, 1–13.

ROUSE, H. 1950 Fundamental principles of flow. *Engineering Hydraulics, Proc. Fourth Hydraulics Conference, Iowa Inst. of Hydraulic Res., June 12–15, 1949* (ed. H. Rouse), pp. 1–135. Wiley.

VERONIS, G. 1963 On the approximations involved on transforming the equations of motion from a spherical surface to the beta-plane. I. Barotropic systems. *J. Mar. Res.* **21**, 110–124.

VERONIS, G. 1973 Large scale ocean circulation. *Adv. Appl. Mech.* **13**, 1–92.

YIH, C. S. 1980 *Stratified flows*. Academic. 418 pp.